ELSEVIER

Computational Materials Science 27 (2003) 191–198

COMPUTATIONAL MATERIALS SCIENCE

www.elsevier.com/locate/commatsci

Second-moment interatomic potential for Al, Ni and Ni–Al alloys, and molecular dynamics application

N.I. Papanicolaou [a,*], H. Chamati [a,1], G.A. Evangelakis [a], D.A. Papaconstantopoulos [b]

[a] *Solid State Division, Department of Physics, University of Ioannina, P.O. Box 1186, GR-45110 Ioannina, Greece*
[b] *Center for Computational Materials Science, Naval Research Laboratory, Washington, DC 20375-5345, USA*

Abstract

We present an interatomic potential for Al, Ni and Ni–Al ordered alloys within the second-moment approximation of the tight-binding theory. The potential was obtained by fitting to the total energy of these materials computed by first-principles augmented-plane-wave calculations as a function of the volume. The scheme was validated by calculating the bulk modulus and the elastic constants of the pure metals and alloys that were found to be in fair agreement with the experimental measurements. In addition, we performed molecular-dynamics simulations and we obtained the thermal expansion coefficient, the temperature dependence of the atomic mean-square displacements and the phonon density of states of the compounds. Despite the simplicity of the model, we found satisfactory agreement with the available experimental data.

Keywords: Interatomic potentials; Elastic constants; Molecular-dynamics simulations; Thermal expansion; Vibrations; Phonons; Aluminum; Nickel; Nickel–aluminum alloys

1. Introduction

In recent years there is an increasing interest in the investigation of the thermodynamic and structural properties of Ni–Al alloys for high temperature applications [1]. It is recognized that first-principles calculations and simulations are superior in studying these properties, but they are computationally expensive, so they are restricted to short time scales and to a few hundred atoms. For larger systems and longer time scales semi-empirical methods, such as the embedded-atom method (EAM) [2], Finnis–Sinclair potentials [3] and the second-moment approximation (SMA) to the tight-binding (TB) model [4–7] are very efficient. In particular the SMA expression of the total energy is based on a small set of adjustable parameters, which are usually determined by matching the experimental data [7,8] or first-principles results [9–11].

The purpose of this work is to provide a reliable TB-SMA interatomic potential, which can describe with satisfactory accuracy the pure metals Al, Ni,

* Corresponding author. Tel.: +30-26510-98562; fax: +30-26510-98693/45631.
E-mail address: nikpap@cc.uoi.gr (N.I. Papanicolaou).
[1] Permanent address: Institute of Solid State Physics, 72 Tzarigradsko Chaussée, 1784 Sofia, Bulgaria.

0927-0256/03/$ - see front matter
doi:10.1016/S0927-0256(02)00445-7

along with their ordered alloys. Our approach consists in fitting the total energy expression of the TB-SMA method to the augmented–plane–wave (APW) total energy curves of these materials. In order to check the validity of our parameters, we calculated the bulk moduli and the elastic constants of the compounds. Furthermore, we performed molecular-dynamics (MD) simulations at various temperatures and we obtained the temperature dependence of the lattice constants and the atomic mean-square displacements (MSD). Finally, we calculated the phonon density of states (DOS) of metals and alloys and we compared them to the available experimental results.

2. Computational details

The electronic band structure of Al, paramagnetic Ni (both fcc and bcc structures) and their alloys $NiAl_3$, Ni_3Al ($L1_2$ structure), NiAl (B2 structure) was calculated self-consistently using the APW method in the muffin-tin approximation [12]. The calculations were scalar relativistic and used the Hedin–Lundqvist parameterization [13], of the local density approximation (LDA). We used a mesh of 89 and 55 k-points in the irreducible Brillouin zone for the fcc and bcc structures, respectively and 35 k-points for the $L1_2$ and B2 structures. The total energy was computed from Janak's expression [14] for six different lattice constants and the resulting volume dependence of the energy was fitted to a parabolic function [15]. For the sake of simplicity the compound $NiAl_3$ was treated in $L1_2$ structure instead of DO_{11}.

In the TB-SMA model [4–7] the total energy of the system is written as

$$E = -\sum_{i=1}^{N}\left(\sum_{j\neq i} A_{\alpha\beta}\exp\left[-p_{\alpha\beta}\left(\frac{r_{ij}}{r_0^{\alpha\beta}}-1\right)\right] - \left\{\sum_{j\neq i}\xi_{\alpha\beta}^2\exp\left[-2q_{\alpha\beta}\left(\frac{r_{ij}}{r_0^{\alpha\beta}}-1\right)\right]\right\}^{1/2}\right), \tag{1}$$

where the first sum represents a pair-potential repulsive term and the second sum corresponds to the band-structure term. In the above expression N is the total number of atoms, r_{ij} is the distance between atoms i and j of the species α and β, respectively (α, β stand for Al or Ni), and the sum over j is extended up to fifth neighbors. The parameter $r_0^{\alpha\beta}$ is taken equal to the APW equilibrium first-neighbor distance in the pure metals ($\alpha = \beta$) and to an average value in the alloys ($\alpha \neq \beta$). There are 12 adjustable parameters $A_{\alpha\beta}$, $\xi_{\alpha\beta}$, $p_{\alpha\beta}$ and $q_{\alpha\beta}$ in this scheme, that describe the interactions of the pure elements and the alloys. These parameters have been determined by fitting Eq. (1) to the APW total-energy curves as a function of the volume for the two metals and the three alloys. The fits have been performed using the MERLIN package [16].

The bulk modulus of the metals and alloys was calculated by using the method proposed in [15]. The elastic constants were calculated at the experimental lattice constants from the difference in the total energies of the distorted and undistorted lattices [17].

In order to validate the model at various temperatures, using the above interatomic potential, we performed MD simulations for the metals and alloys in the canonical ensemble. All systems were made up of 4000 particles arranged on the appropriate lattice structure. The simulation box contained 20 layers with 200 atoms each and periodic boundary conditions were imposed in space. The equations of motion were integrated by means of the Verlet algorithm and a time step of 5 fs. The system was equilibrated at a desired temperature during 10 ps, while thermodynamic averages were computed over 50 ps trajectories. At each temperature, the value of the lattice constant was adjusted to a value resulting from zero pressure in the system, while the atomic MSDs were determined from local density profiles in the direction normal to the atomic layers. Finally the phonon DOSs, were obtained by Fourier transforming the velocity auto-correlation functions.

3. Results and discussion

In Fig. 1, we show the APW calculated cohesive energies per atom (with opposite sign) of the pure

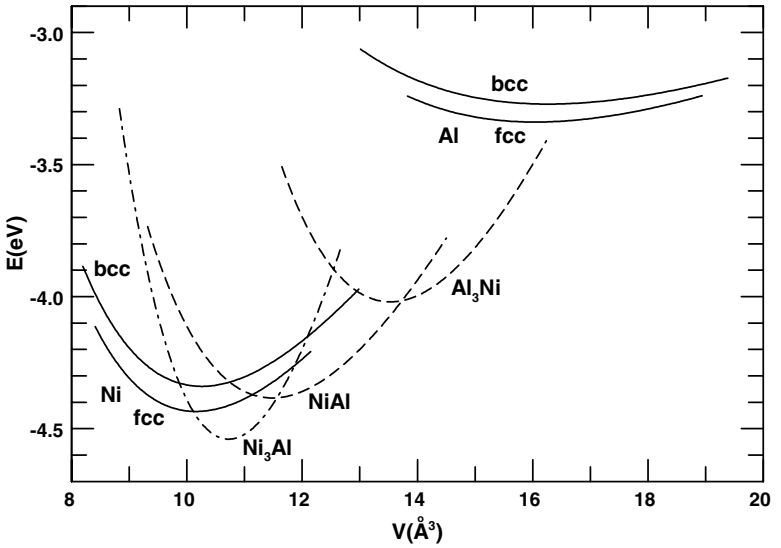

Fig. 1. Cohesive energy per atom (with opposite sign) as a function of volume calculated by the APW method for Al, Al_3Ni, NiAl, Ni_3Al and Ni.

metals Al and Ni (in the fcc and bcc structures) and their ordered alloys $L1_2$–$NiAl_3$, B2–NiAl and $L1_2$–Ni_3Al as a function of the volume. The curves were uniformly shifted, to match at the minimum the experimental value of the respective ground state structure (fcc–Al, fcc–Ni, B2–NiAl, $L1_2$–Ni_3Al, DO_{11}–$NiAl_3$). The determination of the Al–Al and Ni–Ni potential parameters of Eq. (1) has been obtained by fitting to both fcc and bcc respective energy curves of pure metals presented in Fig. 1, while the cross-potential parameters Al–Ni have been obtained by simultaneous fitting to the energy curves of the three ordered alloys. By adopting this procedure, we assume that the Al–Al and Ni–Ni interactions in the alloys are the same as in the respective pure metals. This strategy has the advantage of providing potentials of good quality for pure metals.

The obtained 12 potential parameters of the TB-SMA scheme, along with the theoretical first-neighbor distances, are listed in Table 1. The calculated lattice constants at 0 K within the TB-SMA scheme, together with the respective experimental values at room temperature [18] of metals and alloys, are presented in Table 2. In the same table we provide also the experimental cohesive energy [19–21] we used for the energy shifts in Fig. 1. The differences between the calculated lattice parameters and the corresponding experimental values are 1.4%, 0.5%, 1.1% and 2.9% for Al, NiAl, Ni_3Al and Ni respectively, which are very small except for Ni. The parameters of Table 1 have been used to calculate the bulk moduli and elastic constants of the pure metals and alloys. In

Table 1
Potential parameters of equation (1) for Al, Ni and Ni–Al alloys

Interaction	$\xi_{\alpha\beta}$ (eV)	$A_{\alpha\beta}$ (eV)	$q_{\alpha\beta}$	$p_{\alpha\beta}$	$r_0^{\alpha\beta}$ (Å)
Al–Al	0.9564	0.05504	1.5126	10.9011	2.8310
Ni–Ni	1.4175	0.07415	2.2448	13.8297	2.4307
Ni–Al	1.4677	0.09493	3.8507	10.9486	2.7424

Table 2
Calculated (calc.) and experimental (expt.) [18] lattice parameters, a, along with the cohesive energies, E_c, for Al, Ni [19] and their alloys [20,21]

Compound	a (Å) calc.	a (Å) expt.	E_c (eV) expt.
Al	3.995	4.050	3.339
$NiAl_3$	3.854	–	4.02
NiAl	2.895	2.886	4.50
Ni_3Al	3.526	3.567	4.54
Ni	3.421	3.523	4.435

Table 3
Calculated and experimental values of bulk modulus B and elastic constants for Al, Ni [22] and their alloys [22,23]

Compound	Calculated (GPa)				Experimental (GPa)			
	B	C_{11}	C_{12}	C_{44}	B	C_{11}	C_{12}	C_{44}
Al	71	92	61	58	76	107	61	29
NiAl	222	261	203	80	158	199	137	116
Ni_3Al	232	281	207	96	177	230	150	131
Ni	255	329	218	148	188	261	151	132

The computations were performed within the SMA method.

Table 3, we report these values, along with the available experimental data [22,23]. Considering that we did not fit the C_{ij} (as usually done in atomistic models) the agreement is fairly good, since the largest deviation is about 40%, with the exception of C_{44} for Al.

Furthermore, using the above interatomic potential, we have performed MD simulations at various temperatures. In Fig. 2, we present the computed temperature dependence of lattice parameters of the pure metals and the ordered alloys, from which, we deduce the linear thermal expansion coefficients for these compounds at temperatures (0–600 K). The results are shown in Table 4, along with the corresponding experimental values [19,24]. The accuracy of these quantities is very good. For Al the agreement with the experiment is better than with the previously proposed TB-SMA model [11]. In the case of Ni_3Al, the accuracy is comparable to that obtained by first-principles calculations [25] and better than the TB-SMA potential derived by fitting to several measured

Table 4
Linear thermal expansion coefficient in temperature range of (0–600 K) (in 10^{-6} K^{-1})

Compound	Simulation	Experiment
Al	26.3	23.6
$NiAl_3$	25.0	
NiAl	17.4	10.8
Ni_3Al	15.9	11.8
Ni	15.7	12.5

The experimental data are taken from Ref. [19] for Al and Ni and from Ref. [24] for the alloys.

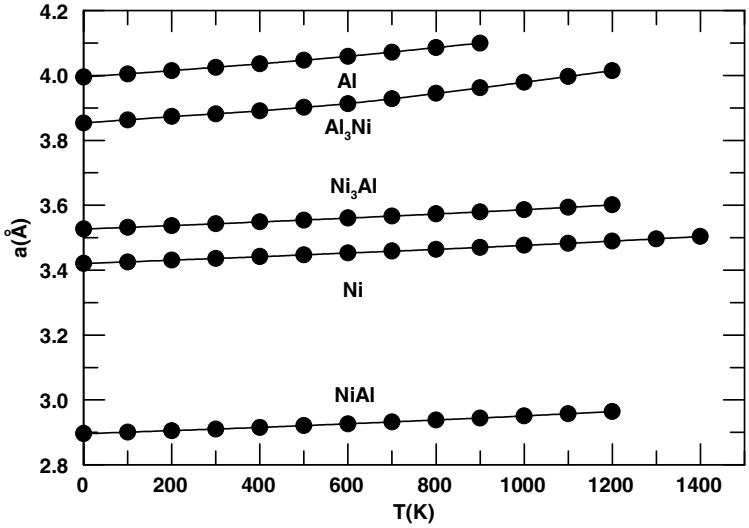

Fig. 2. Temperature dependence of the lattice parameters of Al, Ni and their alloys. The filled circles correspond to the results of the simulations, while the lines are guide to the eye.

data [8] ($a = 19.7 \times 10^{-6}$ K^{-1}). Generally for NiAl, we obtain consistent results with recent simulations using an EAM potential [26], derived from database of experimental and first-principles results in many more structures that we used in the present SMA calculations.

In Fig. 3, we plot the computed atomic MSDs as a function of temperature for the pure elements (solid lines) and the ordered alloys (dashed lines). In the same figure, we also give the experimental values for Al [27] from neutron or X-ray scattering (filled circles), for Ni [28,29] using X-ray diffraction data (open squares and circles, respectively) and for NiAl using electron diffraction [30] or X-ray data [31]. We find excellent agreement between the computed MSDs and the experimental values for Al, while the agreement for Ni is good only at low temperatures (up to 500 K) and in the case of NiAl is better at 110 K [30] than at room temperature [31].

In Fig. 4, we present the computed phonon DOS of Al and Ni at room temperature. In the insets, we also show the experimental spectra. Our phonon spectrum for Al is in excellent agreement with the experimental one, deduced from neutron scattering [32]. Concerning Ni, our model overestimates the maximum frequency and the positions of the two main peaks, by about 1 THz, compared to the experimental measurements using neutron scattering [33]. This may be due to our neglecting the ferromagnetism in our calculations.

In Fig. 5, we present the calculated phonon DOS of the ordered alloys NiAl and Ni_3Al at 300 K. In the insets, we also show the experimental spectra. Comparing the computed phonon spectrum of NiAl to one obtained by neutron scattering [34], we observe reasonable agreement for the maximum frequency, the position of the peaks and the presence of the gap. Nevertheless, our DOS shape is smooth and without the sharp experimental discontinuities, since the computations have been done at room temperature. Furthermore, our phonon spectrum is in fair agreement with the one computed by MD simulations within the EAM potential [35]. In the case of Ni_3Al, we note that the present phonon DOS compares well to the experimental one [36], except for a shift of 1 THz toward higher frequencies in the right part of the spectrum that was also found by first-principles calculation (LDA) [25] (shown in the inset). In

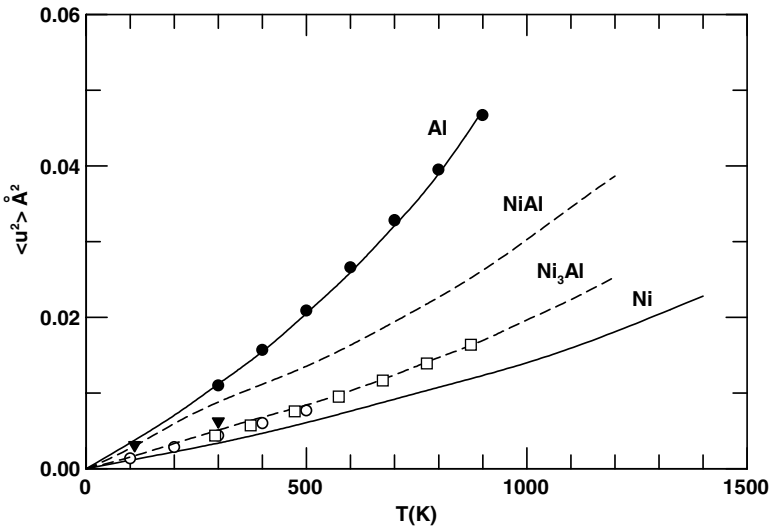

Fig. 3. Mean-square displacements for Al, NiAl, Ni_3Al and Ni. The lines correspond to simulation results. The filled circles are experimental data for Al [27], the open squares and circles indicate the experimental values for Ni [28,29], respectively, while the filled triangles are the experimental data for NiAl [30,31].

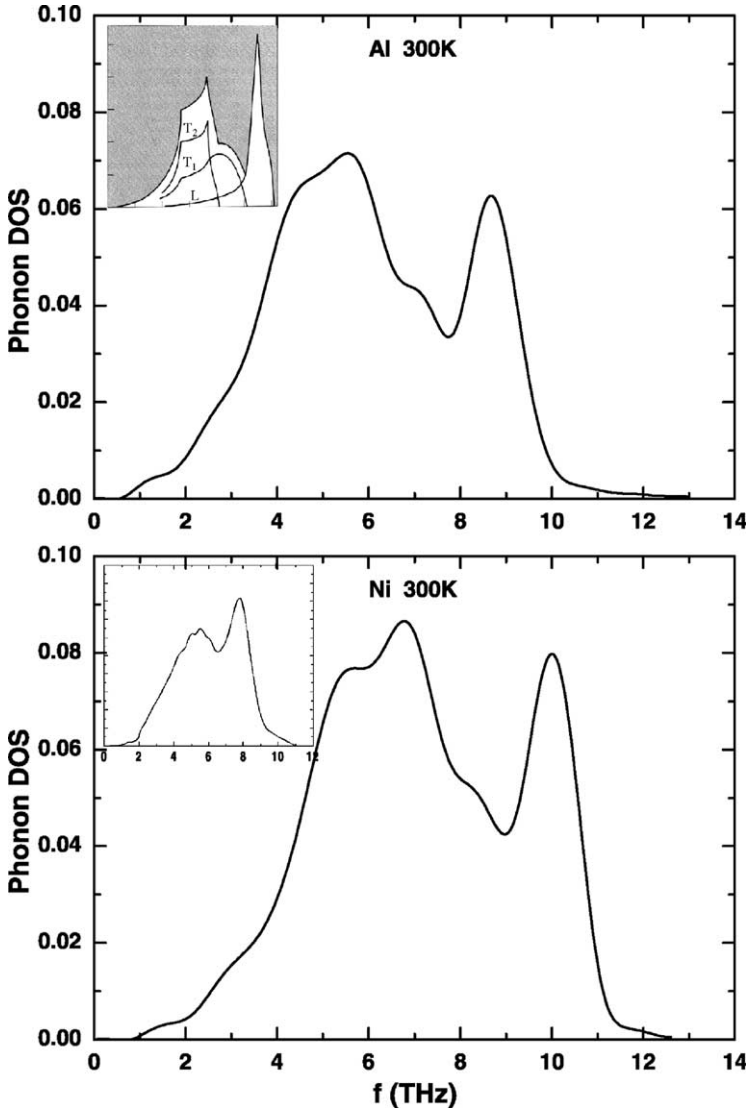

Fig. 4. Phonon DOS (in arbitrary units) of Al and Ni at 300 K. In the insets we show the respective measured spectra [32,33].

addition, the present results are in better agreement with the experimental values than previous TB-SMA computations [8], based on fitting to several experimental data.

4. Conclusion

We presented an interatomic potential of Al, Ni and Ni–Al ordered alloys within the SMA of the TB theory by adjusting the parameters of the energy functional to the first-principles total-energy calculations as a function of the volume. This scheme was applied to calculate the equilibrium lattice constants, the bulk moduli and elastic constants of pure metals and ordered alloys. Our results are generally in good agreement with the experimental values. Furthermore, we used this potential to perform MD simulations, whence we deduced the temperature dependence

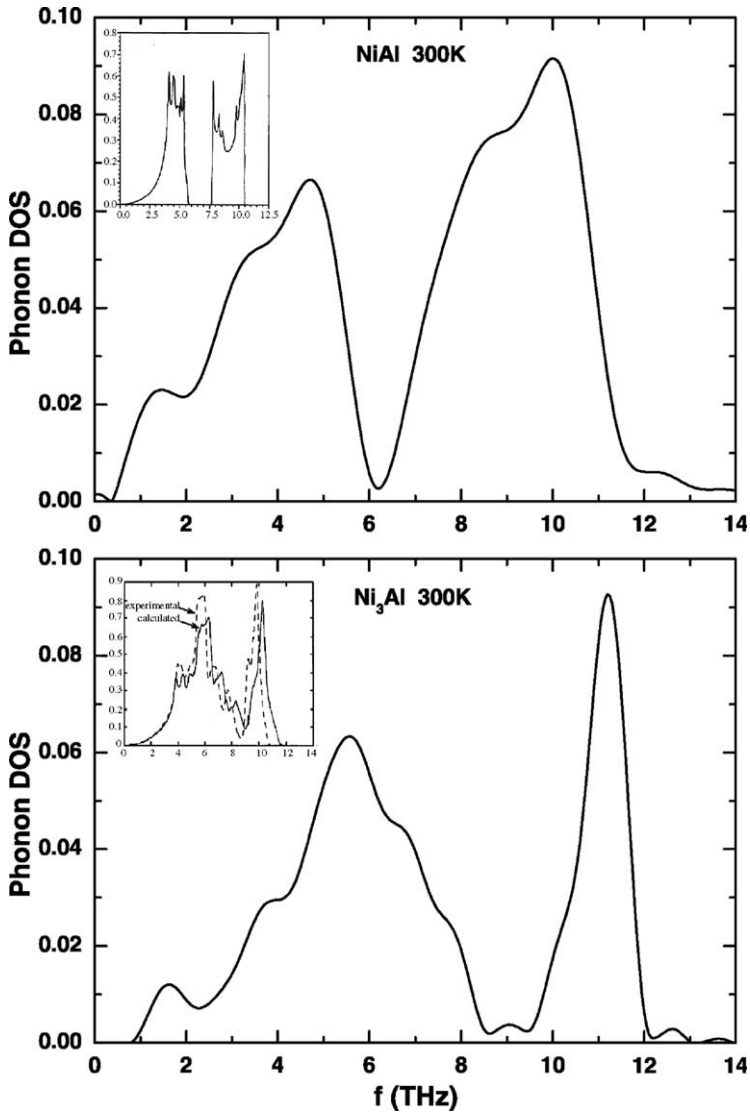

Fig. 5. Phonon DOS (in arbitrary units) of NiAl and Ni_3Al at 300 K. In the insets we show the respective experimental spectra [34,36], as well as the DOS of Ni_3Al from LDA calculations [25].

of the lattice constants and the atomic MSD as well as the phonon DOS at room temperature. Our results appear to reproduce the measured data better than the standard SMA models constructed by fitting to experimental quantities. The advantage of the present model is that, despite its simplicity, not only it describes the pure metals well, but also their ordered alloys and therefore can be useful by providing reliable results in long-scale simulations.

Acknowledgement

This work was supported by European grant HPRN-CT-2000-00038.

References

[1] J.H. Westbrook, R.L. Fleischer (Eds.), Intermetallic Compounds: Structural Applications, vol. 4, John Wiley & Sons, New York, 2000.

[2] M.S. Daw, M.I. Baskes, Phys. Rev. B 29 (1984) 6443; S.M. Foiles, M.I. Baskes, M.S. Daw, Phys. Rev. B 33 (1986) 7983.

[3] M.W. Finnis, J.E. Sinclair, Philos. Mag. A 50 (1984) 45.

[4] F. Ducastelle, J. Phys. (Paris) 31 (1970) 1055.

[5] D. Tomanek, A.A. Aligia, C.A. Balseiro, Phys. Rev. B 32 (1985) 5051.

[6] W. Zhong, Y.S. Li, D. Tomanek, Phys. Rev. 44 (1991) 13053.

[7] V. Rosato, M. Guillope, B. Legrand, Philos. Mag. A 59 (1989) 321.

[8] F. Cleri, V. Rosato, Phys. Rev. B 48 (1993) 22.

[9] G.C. Kallinteris, N.I. Papanicolaou, G.A. Evangelakis, D.A. Papaconstantopoulos, Phys. Rev. B 55 (1997) 2150.

[10] N.I. Papanicolaou, G.C. Kallinteris, G.A. Evangelakis, D.A. Papaconstantopoulos, M.J. Mehl, J. Phys: Condens. Matter 10 (1998) 10979.

[11] N.I. Papanicolaou, G.C. Kallinteris, G.A. Evangelakis, D.A. Papaconstantopoulos, Comp. Mater. Sci. 17 (2000) 224.

[12] L.F. Mattheiss, J.H. Wood, A.C. Switendick, Methods Comput. Phys. 8 (1968) 63.

[13] L. Hedin, B.I. Lundqvist, J. Phys. C 4 (1971) 2064.

[14] J.F. Janak, Phys. Rev. B 9 (1974) 3985.

[15] F. Birch, J. Geophys. Res. 83 (1978) 1257.

[16] G.A. Evangelakis, J.P. Rizos, I.E. Lagaris, I.N. Demetropoulos, Comput. Phys. Commun. 46 (1987) 401.

[17] M.J. Mehl, B.M. Klein, D.A. Papaconstantopoulos, Intermetallic Compounds, in: J.H. Westbrook, R.L. Fleischer (Eds.), Principles, vol. 1, Wiley, New York, 1994, p. 195.

[18] W.B. Pearson, A Handbook of Lattice Spacings and Structures of Metals and Alloys, Pergamon, Oxford, 1967.

[19] C. Kittel, Introduction to Solid State Physics, Wiley-Interscience, New York, 1986.

[20] R. Hultgren, P.D. Desai, D.T. Hawkins, M. Gleiser, K.K. Kelley, Selected Values of the Thermodynamic Properties of Binary Alloys, ASM, Metals Park, OH, 1973.

[21] E.A. Brandes (Ed.), Smithells Metals Reference Book, sixth ed., Butterworths, London, Boston, 1983.

[22] G. Simmons, H. Wang, Single Crystal Elastic Constants and Calculated Aggregate Properties: A Handbook, second ed., MIT Press, Cambridge, MA, 1971.

[23] N. Rusović, H. Warlimont, Phys. Stat. Sol. (a) 44 (1977) 609.

[24] S. Touloukian, R.K. Kirby, R.E. Taylor, P.D. Desai (Eds.), Thermal Expansion, Metallic Elements and Alloys, Volume 12 of Thermophysical Properties of Matter, Plenum, New York, Washington, 1975.

[25] A.V. de Walle, G. Ceder, U.V. Waghmare, Phys. Rev. Let. 80 (1998) 4911.

[26] Y. Mishin, M.J. Mehl, D.A. Papaconstantopoulos, Phys. Rev. B 65 (2002) 224114.

[27] R.C. Shukla, C.A. Plint, Phys. Rev. B 40 (1989) 10337 (references therein).

[28] M. Simerská, Czech. J. Phys. B 12 (1962) 858.

[29] R.H. Wilson, E.F. Skelton, J.L. Katz, Acta Cryst. 21 (1966) 635.

[30] W. Nüchter, A.L. Weickenmeier, J. Mayer, Acta Cryst. A 54 (1998) 147.

[31] P. Georgopoulos, J.B. Cohen, Scr. Metall. 11 (1977) 147.

[32] R. Stedman, L. Almqvist, G. Nilsson, Phys. Rev. 162 (1967) 549.

[33] R.J. Birgenau, J. Cordes, G. Doling, A.D.B. Woods, Phys. Rev. 136 (1964) 1359.

[34] M. Mostoller, R.M. Nicklow, D.M. Zehner, S.-C. Lui, J.M. Mundenar, E.W. Plummer, Phys. Rev. B 40 (1989) 2856.

[35] P. Gumbsch, M.W. Finnis, Philos. Mag. Lett. 73 (1996) 137.

[36] B. Fultz, L. Anthony, L.J. Nagel, R.M. Nicklow, S. Spooner, Phys. Rev. B 52 (1995) 3315.